

Cosmological Aspects of Gamma-Ray Bursts: Luminosity Evolution and an Estimate of the Star Formation Rate at High Redshifts

Nicole M. Lloyd-Ronning

Canadian Institute for Theoretical Astrophysics,
60 St. George St., Toronto, Ontario, M5S 3H8, Canada

lloyd@cita.utoronto.ca

Chris L. Fryer

Theoretical Astrophysics, Los Alamos National Laboratories,
Los Alamos, NM 87544

Enrico Ramirez-Ruiz

Institute of Astronomy, University of Cambridge,
Madingley Road, Cambridge, CB3 0HA, U.K.

ABSTRACT

Using 220 Gamma-Ray Burst (GRB) redshifts and luminosities derived from the luminosity-variability relationship of Fenimore & Ramirez-Ruiz (2000), we show that *there exists a significant correlation between the GRB luminosity and redshift*. In particular, we find that the evolution of the average luminosity can be parameterized as $L \propto (1+z)^{1.4 \pm \sim 0.5}$, where z is the burst redshift. We discuss the possible reasons behind this evolution and compare it to other known sources that exhibit similar behavior. In addition, we use non-parametric statistical techniques to independently estimate the distributions of the luminosity and redshift of bursts, accounting for the evolution (in contrast to previous studies which have assumed that the luminosity function is independent of redshift). We present these distributions and discuss their implications. Most significantly, we find a co-moving rate density of GRBs that continues to increase to $(1+z) \gtrsim 10$. From this estimate of the GRB rate density, we then use the population synthesis codes of Fryer et al. (1999) to estimate the star formation rate at high redshifts, based on different progenitor models of GRBs. We find that no matter what the progenitor or population synthesis model, *the star formation rate increases or remains constant to very high redshifts ($z \gtrsim 10$)*.

1. Introduction

A luminosity function and redshift distribution are among the most sought after quantities for any class of astrophysical objects. From QSOs, to various types of galaxies, to supernovae, etc., these distributions provide important insights not only into the physics of the individual objects themselves, but also into the evolution of matter in our universe. A luminosity function is a measure of the number of objects per unit luminosity and therefore is intimately connected to the energy budget (e.g. mass, rotational energy, etc.) and the physical parameters determining the emission mechanism (e.g. density, magnetic field, etc.) of the objects. On the other hand, the co-moving rate density, a measure of the number of events occurring per unit co-moving volume and time, provides a census of the number of objects formed at a given redshift and can help us understand object/structure formation in its various stages of evolution. Often, when doing large statistical studies of a particular class of objects, the luminosity function and redshift distribution are assumed to be independent quantities; that is, the sources' luminosity function is assumed to be the same for all redshifts. This makes the analysis easier when one has limited information (e.g. significant data selection effects) obscuring a direct interpretation of the measured distributions of luminosity and redshift. However, it has been shown that this assumption is not valid for many astrophysical objects (for example, see §5.1.3)

In this paper, we examine the evolution of the luminosity function, as well as the co-moving rate density of Gamma-Ray Bursts. Currently, there are on the order of about 20 bursts with measured redshifts (see Jochen Greiner's homepage at: <http://www.aip.de/~jcg/grb.html> for a compilation of all observed afterglow results); a histogram of all the redshifts as of July, 2001 is shown in Figure 1. The gamma-ray burst community has been very successful in gaining a working understanding of GRBs from these (and a few other) individual bursts. By studying the prompt and especially afterglow emission in great detail for a few GRBs, some important generalizations have been made. For example, it was clear from the very first bursts with measured redshifts that the GRB luminosity function is *not* very narrow and in fact exhibits a rather large dispersion (unless otherwise stated, by "luminosity", we mean luminosity modulo a beaming factor $d\Omega$). Through indirect evidence (extinction estimates, position in host galaxy, possible SNe in light curves; see §5 for further discussion), it can be inferred that many GRBs are associated with star forming regions which helps constrain certain progenitor models (see, e.g., Meszaros, 2001, and references therein).

However, there are still a number of unanswered questions that can only be addressed through larger scale population studies of GRB luminosities and redshifts. Because GRBs are most likely associated with some sort of compact object(s) (e.g. a very massive star or two compact objects such as neutron stars or black holes merging), the luminosity distribution

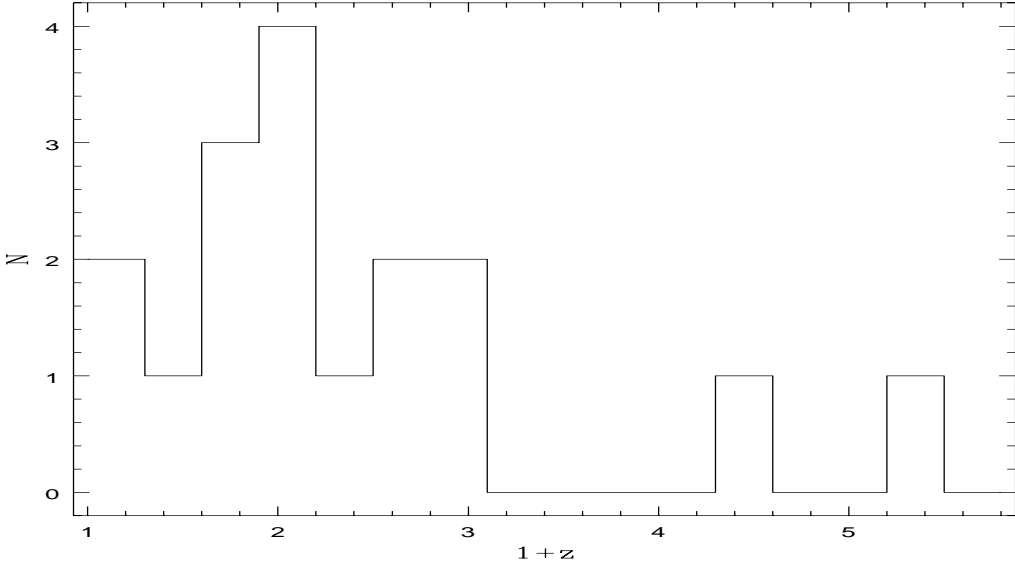


Fig. 1.— Histogram of seventeen bursts with confirmed measured redshifts.

may help us eventually constrain the parameters on which the energy output depends (such as mass and angular momentum), and ideally help us understand the nature of the progenitor. If this luminosity function evolves, this not only provides additional insight into the physical parameters fundamental to the gamma-ray burst, but may help shed light on the evolution of the GRB host environment. Finally, because of a probable connection to massive stars (in *both* the collapse and merger models), the GRB co-moving rate density can provide novel information about the rate of star formation in our universe.

Therefore, getting a handle on the GRB luminosity function and rate density could have important consequences for understanding not only GRBs themselves, but other astrophysical problems as well (particularly, determining the star formation rate at high redshifts). But because the GRB luminosity function is not a δ -function, we cannot use its flux as a standard candle from which to infer a redshift to the source (for example, see Figure 1 in Lloyd et al., 2000, which shows the dispersion in the isotropic equivalent energy for those bursts with measured redshifts). At first glance, it appears that direct measurements of a large number of redshifts to bursts (e.g. by HETE-2 and Swift) with careful accounting of the detector selection effects is the only way to get a handle on the burst density distribution and luminosity function.

However, recently it has been suggested that there exist other types of standard candle or Hubble-type relationships in GRBs, from which a redshift can be inferred from a common

GRB observable. For example, Norris, Marani, & Bonnell (2000) report a positive correlation between spectral lag and luminosity - from 6 bursts with measured redshifts, the higher luminosity bursts show more of a delay between the high energy and low energy pulses than do weaker bursts. Fenimore & Ramirez-Ruiz (2000; hereafter, FRR) were the first to report a relation between the bursts variability, V , - defined by the "spikiness" of the light curve - and the luminosity for 8 bursts with measured redshifts (see also Reichart et al., 2000, for further analysis of this relation). From this relationship, they estimated luminosities and redshifts to 220 GRBs with a peak flux above $1.5\text{ph}/\text{cm}^2/\text{s}$. This was done by computing the variability (see FRR for exact definition) of each bursts' light curve, then inferring the luminosity from the determined correlation, and finally computing a redshift (assuming some cosmological model). Their procedure is described in further detail below.

The goal of this paper is to test for correlation between luminosity and redshift in the FRR data, estimate the bivariate GRB distribution of luminosity and redshift $\Psi(L, z)$, and then use this distribution to place constraints on the star formation rate at early times. It is important to point out that because of the flux threshold in the FRR sample, there is a strong truncation of the data produced in the $L - z$ plane (see §2.2 and 3), which renders it difficult to estimate the underlying parent (or intrinsic) distributions of L and z , or any intrinsic correlation between them. FRR attempt to account for this truncation threshold by first assuming *independence* of the variables L and z , and then constructing redshift-luminosity bins parallel to the L and z axes. They estimate a luminosity function $\phi(L)$ in each redshift bin, and then find a function $\rho(z)$ that causes the $\phi(L)$ curves in each redshift bin to fall on top of one another or match each other. Using this method, FRR find $\phi(L) \propto L^{-2.3}$ and $\rho(z) \propto (1 + z)^{3.3 \pm 0.3}$. We emphasize that their method *implicitly assumes no luminosity evolution*¹.

In this paper, we show that if the $L - V$ luminosity indicator is valid, it leads to a GRB luminosity function that depends on redshift. We use robust non-parametric statistical techniques to estimate the significance of this correlation given the selection threshold. Accounting for this luminosity evolution, we then investigate the density distribution and shape of the luminosity function for this sample, and use this information to make an estimate of the star formation rate at high redshifts. The organization of this paper is as follows: In §2, we give a brief introduction into the nature of the luminosity-variability correlation, and discuss the data sample we use in our study. In §3, we describe the statistical techniques employed to account for the flux threshold truncation and then apply these to our sample. In §4, we describe our results. We find that the burst luminosity L is significantly correlated

¹We do point out that when *assuming* a density distribution proportional to the star formation rate, FRR do find the luminosity function must evolve, although do not quantify this.

with redshift z and can be parameterized by $L \propto (1+z)^{\sim 1.4}$. Accounting for this correlation, we estimate the redshift distribution as well as the distribution of a measure of luminosity (with redshift dependence removed). In particular, we find that the co-moving rate density of GRBs increases to very high redshifts. In §5, we discuss the implications of GRB luminosity evolution and meaning of the luminosity and density distributions. We then use population synthesis codes developed by Fryer et al.(1999) to estimate the star formation rate at high redshift from the GRB co-moving rate density. We find that the star formation rate increases at high redshift for merger models, and either increases or remains approximately flat at high redshift for collapsar models. Therefore, no matter what the GRB progenitor we use, we find the star formation rate continues to increase (or at the very least remains constant) beyond a redshift of $(1+z) \sim 3$. In §6, we summarize and present our main conclusions.

2. The Luminosity-Variability (L-V) Correlation

As described in the introduction, Fenimore & Ramirez-Ruiz (2000) have found a correlation between the GRB luminosity (in the 50-300 keV energy range²), and the light curve “variability” for 8 bursts with measured redshifts (models for the physical mechanism behind this correlation can be found in Plaga, 2001, Ioka & Nakamura, 2001, Kobayashi et al., 2001, and Ramirez-Ruiz & Lloyd-Ronning, 2002). This relationship is confirmed by Reichart et al. (2000) using a slightly different measure of variability as well as other subtle differences as described in §3 of FRR. In their most recent analysis, FRR find that the luminosity L is proportional to a measure of variability V of the GRB lightcurve (a further description of variability is given in §2.2 below; for the exact definition, see equation 2 of FRR) to a power $1.57 \pm \sim 0.5$.³ Because V is a readily measured quantity from the bursts’ light curves, the $L - V$ relation serves as a luminosity indicator for those bursts which *do not* have measured redshifts. Once the luminosity is found from this relationship, a redshift can then be computed (under the assumption of some cosmological model).

As seen in the papers of FRR and Reichart et al. (2000), the correlation has significant scatter. However, although the exact power-law relationship is not well established, its existence appears to be robust. For example, Schaefer (2001) finds a relationship between

²Using the “bolometric” gamma-ray luminosity gives similar results, however.

³Earlier versions of the paper which used a different degree of smoothing of the light curve, and therefore a different definition of the variability V_* gave $L \propto V_*^{3.35(+2.45,-1.15)}$. It is important to point out that no matter which luminosity indicator we use (with variability defined as V or V_*), all of our results remain qualitatively similar.

pulse lag and variability in the BATSE data which is predicted if both the lag-luminosity and variability-luminosity correlations are real. In addition, several authors have found evidence that appears to support this relationship in the GRB light curve power density spectrum (PDS). Pozanenko (private comm.) finds a correlation between the GRB luminosity and “RMS variability”, where the RMS variability is the integral of the PDS above some fixed frequency (and therefore a measure of the contribution of high frequency emission to the lightcurve). Similarly, Beloborodov et al. (2000) find a positive correlation between the PDS spectral index and luminosity for bursts with redshifts. The spectrum is shallower for brighter bursts (implying more high frequency emission for brighter bursts), which is also at least qualitatively consistent with the existence of the luminosity-variability correlation. As mentioned above and as we show below, despite the scatter in the FRR luminosity-variability relation, the qualitative nature of our results are not sensitive to the precise value of the $L-V$ correlation index. In this section we describe the data sample obtained from this correlation, which we use in our investigation.

2.1. Data

The data we use in this analysis is from Table 2 of FRR, which lists the peak flux in the 256ms time bin and from 50-300keV, the T_{90} duration, the measure of the variability, the determined redshift and luminosity from the empirically determined relationship, for 220 BATSE bursts. From the burst time profile, they calculate a measure of variability, defined in their equation (2). The variability is most easily understood as the degree of “spikiness” of the light curve - that is, the sum of mean square difference between the actual counts and a smoothed light curve. Their definition of variability accounts for time dilation and the fact that the time scale in a GRB light curve is energy dependent (Fenimore et al., 1995) as well as for the presence of Poisson noise (the expected value of V for pure Poisson noise is zero). Then, given the relationship between luminosity and variability presented in their paper, $L/d\Omega = 3.1 \times 10^{56} V^{1.57} \text{ erg s}^{-1}$, they calculate a luminosity for the 220 BATSE GRBs in their sample. Finally they solve for redshift through the relation

$$L/d\Omega = f_{256} \langle E \rangle \left[\int_0^z (c/H_o) \frac{dz}{\sqrt{\Omega_\Lambda + \Omega_m(1+z)^3}} \right]^2 \quad (1)$$

where f_{256} is the peak photon flux on the 256 ms timescale and in the energy range 50 – 300 keV, $\langle E \rangle$ is the average energy of the spectrum obtained by integrating the spectrum over the 50 – 300 keV range, c is the speed of light, and they use $H_o = 65 \text{ km/s/Mpc}$, $\Omega_m = 0.3$,

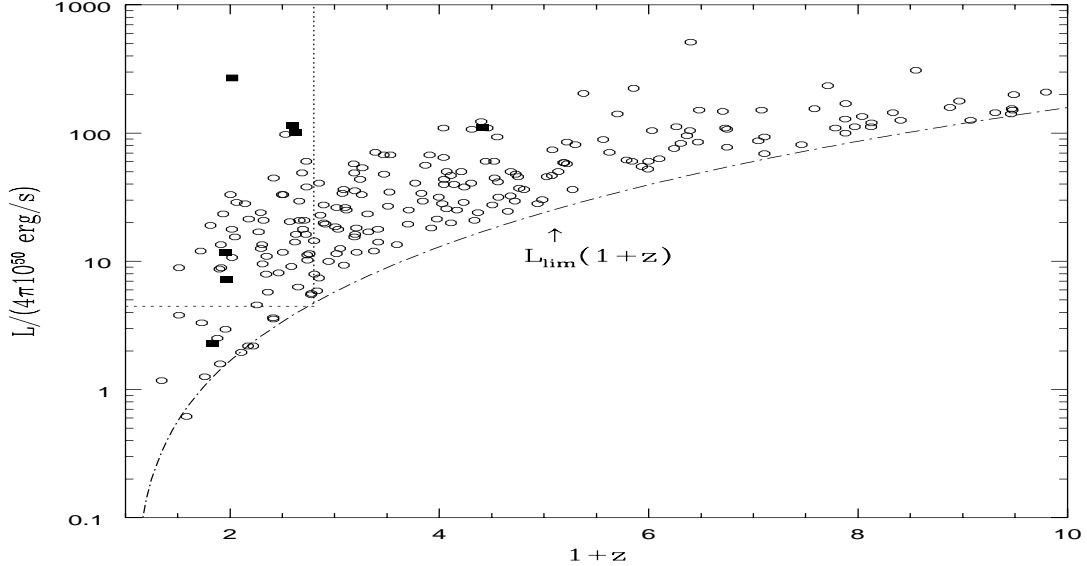


Fig. 2.— Normalized luminosity vs.redshift for 7 bursts (squares) with confirmed redshift measurements from which the L-V correlation of FRR was derived, and the 220 BATSE bursts (circles) on which this correlation was applied to obtain luminosities and redshifts (see §2 of text). The dot-dashed line is the truncation limit as a result of the peak flux threshold in the FRR sample. The dotted vertical and horizontal lines show a representative “associated set” for one particular burst as used in our statistical methods described in §3.

$\Omega_\Lambda = 0.7$.⁴ Because of the subtleties of the dependence of the light curve on redshift (through time dilation and the dependence of pulse width on energy), the redshift is actually obtained through an iterative procedure as described in §4 of FRR. Note that they choose an upper limit to the redshift of 12.

The FRR sample is chosen to have peak fluxes above the threshold $f_{256} = 1.5 \text{ ph/cm}^2/\text{s}$, which defines a limiting luminosity as a function of redshift according to the equation above. The data (circles) and their truncation limit as defined by this equation are shown in Figure 2, where the solid squares denote those bursts with measured redshifts; the horizontal and vertical lines are relevant for our statistical methods and are explained in §3. The truncation places an important restriction on the amount of information we can obtain from the data. Because our goal is to learn about the *parent* (or intrinsic) distributions of L and z (e.g.

⁴Note the factors of $(1+z)^2$ present in the usual definition of luminosity distance and explicitly absent in the expression above are contained in the $\langle E \rangle$ calculation; see FRR for a discussion of this luminosity distance issue.

the distributions without truncation), we must account for the truncation limit in some way. Fortunately, because the threshold is so well defined, we can use previously developed non-parametric techniques to gain full information on the underlying distributions from the observed distributions and knowledge of the truncation limit.

3. Statistical Techniques

Our goal is to estimate the bivariate distribution of luminosity and redshift, $\Psi(L, Z)$, where $Z = 1 + z$. We do not assume L and Z are independent. However, without loss of generality, we can write $\Psi(L, Z) = \rho(Z)\phi(L/\lambda(Z))/\lambda(Z)$, where $\phi(L/\lambda(Z))$ is the luminosity function, and $\lambda(Z)$ parameterizes the correlation between L and $1 + z$. Trying to estimate *correlations between and distributions of* variables which suffer from selection effects without accounting for the truncation can lead to drastically false conclusions. Obviously, if one blindly computed the correlation between L and Z without accounting for the severe truncation present in the $L - Z$ plane due to the lower flux threshold as seen in Figure 2, one would find they are highly correlated. Of course, this would be a result of the truncation itself, and not reflect any real physics in the underlying distributions. The point is that we need some way of learning about the data not observed (falling below the truncation line) from the data that is observed and from the truncation itself.

There are simple, straightforward ways to estimate the parent distribution of truncated samples of data using maximum likelihood arguments. These methods are based on ideas first put forth by Lynden-Bell (1971) and then further developed by Efron & Petrosian (1992). Treatment of the most general case of multiply-truncated data is discussed in Efron & Petrosian (1999). These non-parametric statistical techniques used a well defined truncation criterion (and the assumption that the observed sample is the one most likely to *be* observed) to estimate the correlation between (if any), and underlying parent distribution of, the relevant observables. We now describe these methods in the context of our particular problem. A particularly lucid explanation of the techniques as applied to quasar data is found in Maloney & Petrosian (1999). These techniques applied to GRB spectral data as well as simulations showing how accurately these methods work can be found in Lloyd & Petrosian (1999) and Lloyd et al. (2000).

3.1. How to Apply These Methods to our Data

Consider a set of observables L_i and Z_i where i indexes the particular burst and in our case i runs from 1 to 220. The luminosity suffers from a lower limit set by the constant flux threshhold in the FRR sample, given by equation (1): $L_{lim}(Z) = L(f_{256} = 1.5\text{ph}/\text{cm}^2/\text{s})$.⁵ For each burst indexed by i , we can define an *associated set* J_i defined as:

$$J_i \equiv \{j : L_j > L_i, L_{lim,j} < L_i\} \quad (2)$$

This creates a truncation parallel to the axes as shown by the horizontal and vertical dotted lines in Figure 2. The associated set is all objects j that could have been observed given i . Now, for each burst i , we can define a rank of z_i in the eligible set:

$$R_i = \#\{j \in J_i : z_j \leq z_i\} \quad (3)$$

We expect R_i to be uniformly distributed between 1 and N_i , where N_i is the number of points in J_i . To estimate the degree of correlation between L and $Z = 1 + z$, we can construct a version of Kendall's τ statistic. Let $T_i \equiv (R_i - E_i)/V_i$, where $E_i = (N_i + 1)/2$, and $V_i = (N_i^2 - 1)/12$. Then,

$$\tau = \frac{\sum_i (R_i - E_i)}{\sqrt{\sum_i V_i}} \quad (4)$$

This τ statistic is normally distributed about a mean of 0 with a standard deviation of 1 (Efron & Petrosian, 1992). Hence, a τ of -4 implies a 4σ anti-correlation between the variables at hand. This is similiar to the usual Kendall's τ statistic defined as:

$$\tau_K = \frac{pos - neg}{\sqrt{pos + neg + ytie} \sqrt{pos + neg + xtie}} \left(\frac{4N + 10}{9N(N - 1)} \right)^{-1} \quad (5)$$

where pos denotes the number of positive comparisons (the “position” - meaning whether its greater than or less than - of x_i relative to x_j is the same as the “position” of y_i relative to y_j), neg denotes the number negative comparisons (the relative positions of the x 's and y 's are different), tie denotes $x_i = x_j$ ($xtie$) or $y_i = y_j$ ($ytie$), and N is the number of data points. This is also normally distributed about 0 with a standard deviation of 1. The difference between τ and the usual Kendall's τ_K is that, in the former case, points are compared only if they are within eachother's truncation limits (in other words, only points within associated sets are compared). For example, if y_j fell below the lower limit of y_i , these two points would not be compared. Once the existence of the correlation is established, it is easy to

⁵ Alternatively, we can say that the redshift z suffers from an upper limit, given by the inversion of equation 1. Either way we do the problem gives us equivalent answers.

parameterize it in some quantitative way. One needs only to transform one of the variables, say L , as $L \rightarrow L' = L/\lambda(Z)$, where $\lambda(Z)$ can be written as $\lambda(Z) = (1+z)^\alpha$, and then vary α until $\tau = 0$.

It is also simple to estimate the underlying parent distributions of the variables at hand once the correlation is known. This method relies on the assumption of independence of variables, so we must apply this method to the uncorrelated variables L' and $Z = 1+z$. For uncorrelated variables L' and Z , we again rely on finding the associated set for each variable and the number of points in that set N'_i . Then, the cumulative distribution Φ of L' , which is the number of bursts with L' greater than L'_i , is given by the simple formula (Lynden-Bell, 1971, Efron & Petrosian, 1992, Petrosian, 1993):

$$\ln\Phi(L_i) = \sum_{j < i} \ln\left(1 + \frac{1}{N_j}\right) \quad (6)$$

For each point indexed by j , a truncation parallel to the axes is made and a weight $1/N_j$ based on the number of points in the associated set is assigned to that data point.

Simulations demonstrating how well these techniques work at determining underlying correlations and the distributions given a well defined truncation are in published in the Appendices of Lloyd and Petrosian (1999) and Lloyd et al. (2000). There, we simulate correlated parent distributions, invoke a truncation representing some observational selection effect, and define an observed sample by those points that survived truncation. We then 1) recover the correlation present in the parent sample even when the truncation produces an “observed” correlation of the opposite sign, and 2) fully recover the distributions of the underlying parent samples.

4. Results

We apply the statistical techniques described above to the 220 FRR bursts shown in Figure 2. We find that there is a significant ($> 10\sigma$) correlation between the underlying parent distributions of luminosity and redshift in this sample, when accounting for the truncation. In other words, the null hypothesis that luminosity is independent of redshift is rejected at the 10σ level. The functional form of the correlation can be conveniently parameterized by $\lambda(Z) \propto (1+z)^{1.4 \pm 0.2}$, in the sense that $L' = L/\lambda(Z)$ is uncorrelated with redshift (the error bars here represent the statistical error for this data set; see §4.1 for a discussion of the error due to the scatter in the L-V relation). The function $\lambda(Z)$ therefore represents a sort of

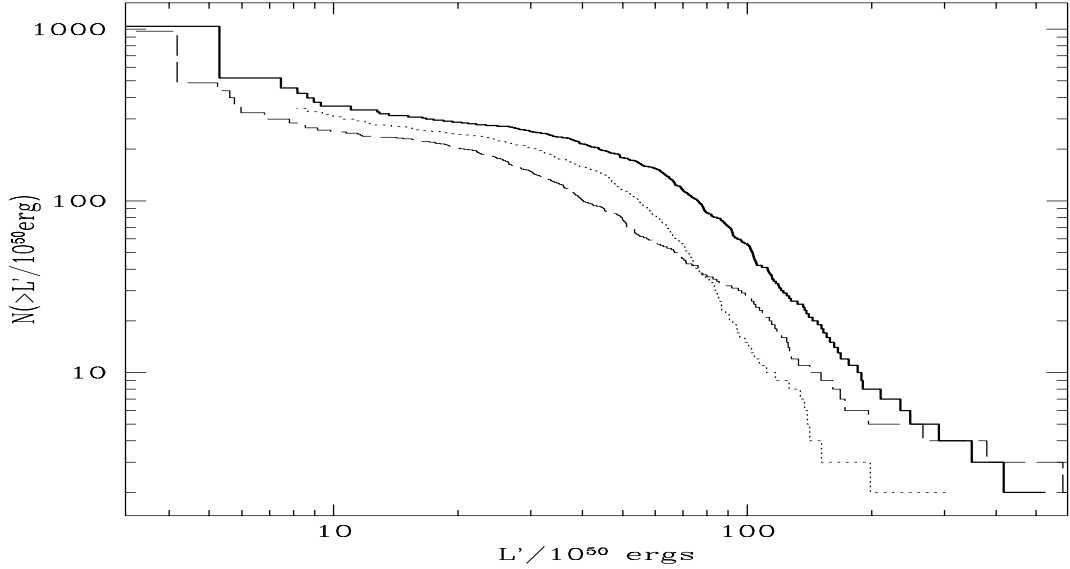


Fig. 3.— Cumulative L' distribution $N(>L')$ as a function of L' : for 220 bursts in the FRR sample, accounting for the flux threshold selection limit. As described in §3 and 4, L' is the luminosity with the redshift dependence $(1+z)^{1.4}$ removed: $L' = L/(1+z)^{1.4}$. The heavy solid line is for the best fit $L - V$ relation, while the dotted and dashed lines are for the lower and upper bounds to the relation, respectively (see §4.1 in text).

average luminosity as a function of redshift⁶. This is the first time luminosity evolution has been demonstrated. To the best of our knowledge, all results published previously regarding the luminosity and redshift distributions of GRBs, which have implicitly assumed no luminosity evolution in their analyses (e.g. FRR, Schmidt 2001, and others). We again point out that our luminosity is actually modulo a burst beaming factor $d\Omega$, so that this correlation may be an indication of evolution of *either* the actual luminosity or the burst jet angle. We address this issue in the discussion section below.

Since we have an estimate of the correlation present between L and Z , we can independently compute the distributions of the uncorrelated variables L' and Z . These distributions are presented in various formats in Figures 3 through 7. Figure 3 shows the cumulative

⁶Although it may eventually be useful to try other functions of luminosity evolution other than a simple power law, such detailed analyses are not necessary for the purposes of this paper and should wait until the luminosity-variability correlation is more quantitatively sound. For our purposes, the most important result is that the GRB luminosity *does* evolve with redshift - we address the meaning and robustness of this result in the text.

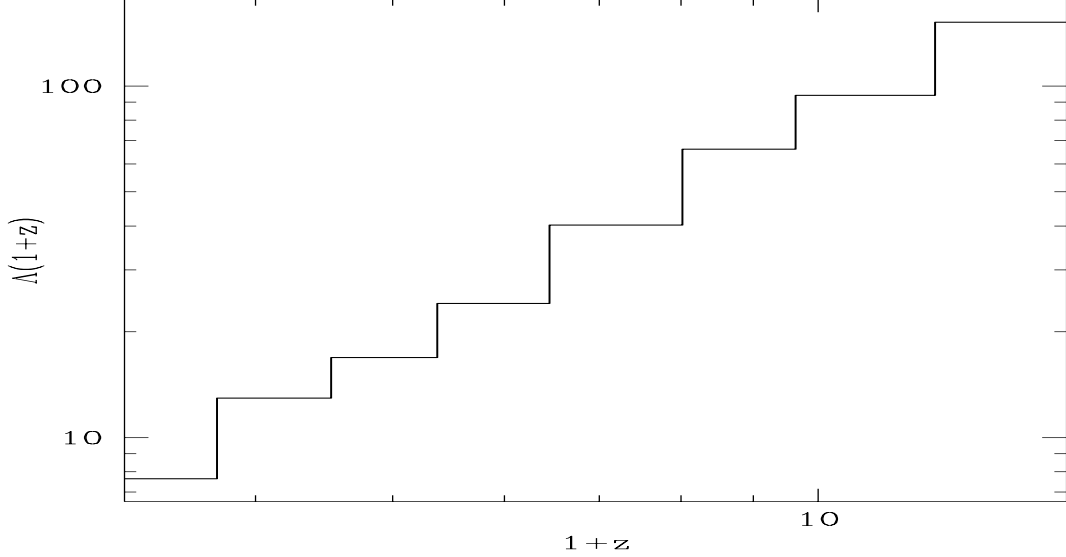


Fig. 4.— Total emitted luminosity as a function of redshift for the 220 GRBs in the FRR sample, using luminosities and redshifts for the best fit L-V relation.

distribution of $L' = L/\lambda(Z) = L/(1+z)^{1.4}$ for the best fit $L - V$ relation (solid line) as well as for the lower (dotted line) and upper (dashed line) bounds to this relation (see §4.1). We have tried several fits to this cumulative luminosity function (for the solid line) with the following results: a single power-law fit to the data yields $N(> L') \propto L'^{-1.28 \pm 0.02}$. Fitting a double power law to this curve we find indices -0.51 and -2.33 above and below respectively a break of $L' = 5.9 \times 10^{51}$ ergs. These results yield a *differential* luminosity function dN/dL' with indices ~ -1.5 in the shallower parts (low L') to ~ -3 in the steepest parts (higher L'). This is similar to the luminosity function found by FRR, who find a differential luminosity distribution (without accounting for luminosity evolution) of $dN/dL \propto L^{-2.3}$ for this sample. However, because L' is not the actual luminosity of the burst, but rather the luminosity with the redshift evolution removed, the interpretation and comparisons of the luminosity function are not straightforward. Another, perhaps more useful, quantity to examine is the total luminosity emitted at a given redshift. The total luminosity emitted at a given redshift is defined as $\Lambda(Z) = \int_0^\infty L \Psi(L, Z) dL = \rho(Z) \int_0^\infty \phi(L/\lambda(Z)) L (dL/\lambda(Z)) = \rho(Z) \lambda(Z) \int_0^\infty \phi(L') L' dL'$. So that $\Lambda(Z) \propto \rho(Z) \lambda(Z)$. As seen in Figure 4, this function strongly increases with redshift (with a slope of about 2) with no apparent turnover out to a redshift of at least 10.

Figure 5 shows the cumulative distribution of redshift, $N(< Z)$; the solid line is for redshifts from the best fit value of FRR's $L - V$ relation, while the dotted and dashed lines are the distributions for the lower and upper bounds to the L-V relation, respectively. It

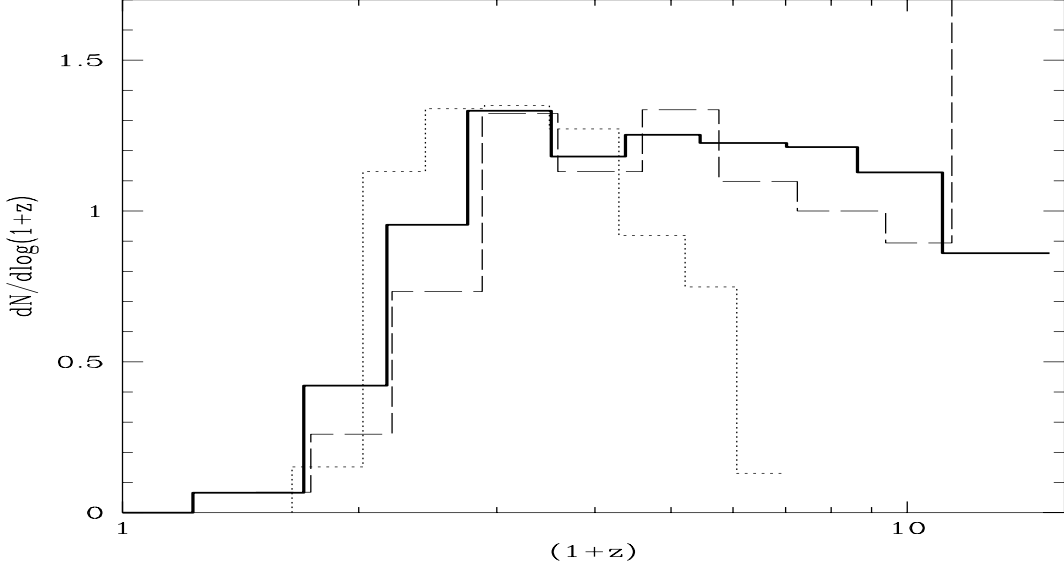


Fig. 5.— Differential distribution of gamma-ray bursts in the FRR sample as a function of redshift. The heavy solid line is for the best fit $L - V$ relation, while the dotted and dashed lines are for the lower and upper bounds to the relation, respectively (see §4.1 in text).

is evident that the distribution of GRBs increases with increasing z . In Figure 6, we show the differential distribution dN/dZ of GRBs as a function of redshift. From this differential number distribution, we can derive a co-moving rate density of gamma-ray bursts through the relation:

$$\rho(Z) = \frac{dN}{dZ}(1+z)\left(\frac{dV}{dZ}\right)^{-1}, \quad (7)$$

where V is volume, and

$$dV/dZ = 4\pi(c/H_o)^3 \left(\int_1^{1+z} \frac{d(1+z)}{\sqrt{\Omega_\Lambda + \Omega_m(1+z)^3}} \right)^2 \frac{1}{\sqrt{\Omega_\Lambda + \Omega_m(1+z)^3}}. \quad (8)$$

The additional factor of $(1+z)$ in equation (7) comes from the fact that we are measuring a *rate* and so must account for cosmological time dilation. We have plotted the density distribution in Figure 7 for $\Omega_\Lambda = 0.7$, $\Omega_m = 0.3$, and $H_o = 65 \text{ km/s/Mpc}$, where we have arbitrarily normalized the curve so that $\rho(Z) = 1$ at $Z = 1$. Note that the density sharply rises as $\sim (1+z)^3$ to a redshift of about 2, and then rises at a slower rate after that ($\sim (1+z)^1$) to at least a redshift of 10. In §5.2, we will use the GRB redshift distribution to place limits on the global star formation rate at high redshifts.

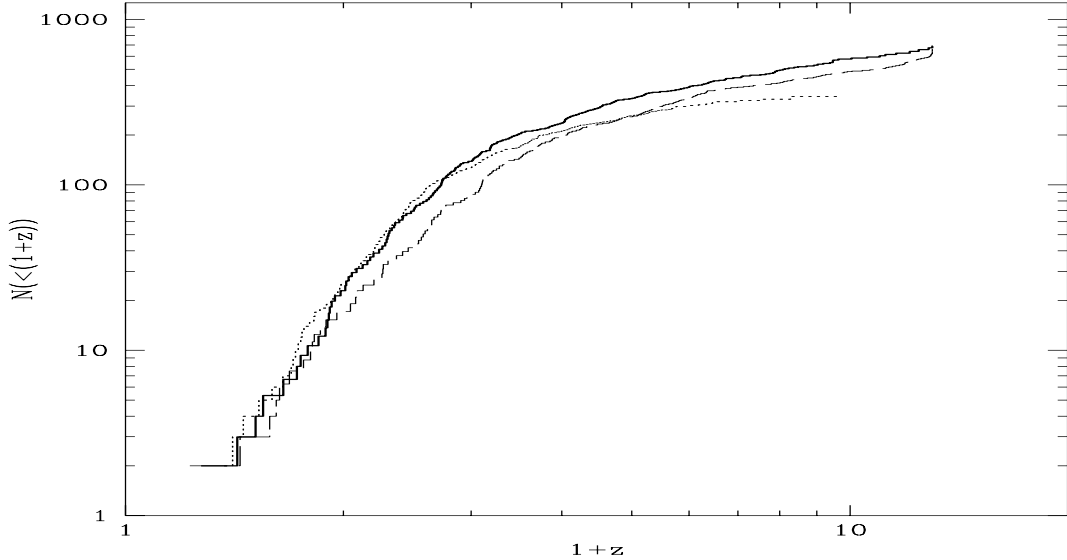


Fig. 6.— Cumulative distribution $N(< 1 + z)$ as a function of redshift for the 220 bursts in the FRR sample, accounting for the truncation threshold in the L-z plane. The solid line represents the cumulative distribution for the best fit value of the L-V relation. The dotted and dashed lines are the distributions for the lower and upper bounds to the L-V relation, respectively (see §4.1 in text).

4.1. Robustness of the Results

Because there is a significant amount of scatter in the $L - V$ relationship, it is important to discuss how our results change as a function of the power law index in the $L - V$ correlation. First, we have repeated our analysis using tables of redshifts and luminosities from the two bounding relationships in FRR: $L \propto V^{1.03}$ and $L \propto V^{2.05}$. In both cases we find that the null hypothesis of no luminosity evolution is rejected with very high significance - 6.5σ and 6σ for the lower and upper bounds, respectively. We can parameterize the evolution in these cases as $L \sim (1 + z)^{1.3 \pm 0.2}$ for the lower bound and $L \sim (1 + z)^{1.9 \pm 0.2}$ for the upper bound. In addition, we have attempted to account for the dispersion in the L-V relationship in the following way: for a given observed variability V , we draw a value for the luminosity from a uniform distribution covering the total possible range of luminosities allowed by the bounding power laws of the L-V relation. We then compute the corresponding redshift (given our cosmological model described above). We then test whether the null hypothesis of no correlation between luminosity and redshift holds. Once again, we find that it is rejected with high significance ($\sim 6\sigma$), and that the evolution can be parameterized as $L \sim (1 + z)^{1.7 \pm 0.4}$.

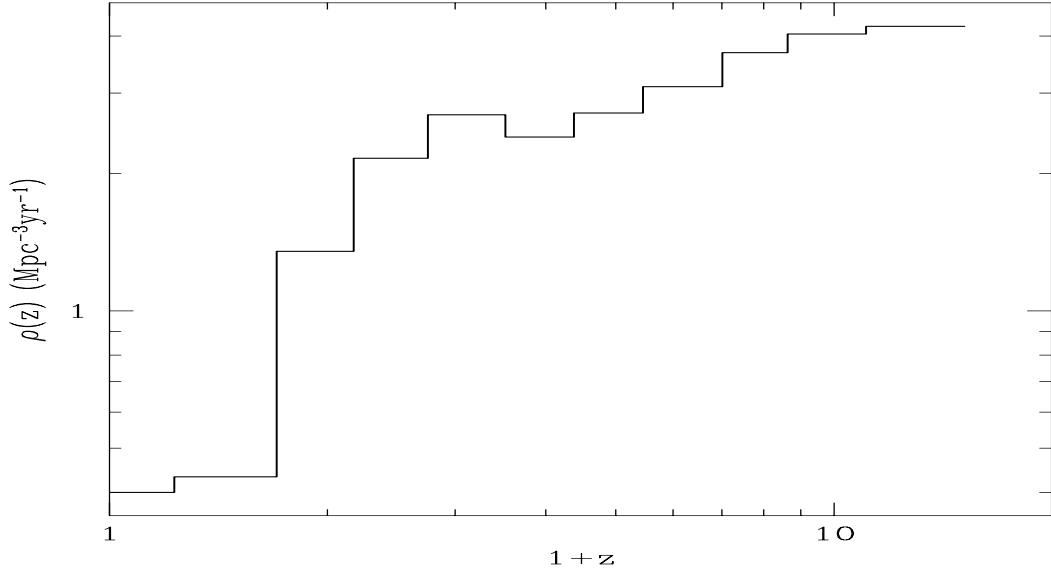


Fig. 7.— The co-moving GRB rate density $\rho(1+z)$ for our sample. We have arbitrarily normalized the curve to ~ 1 at $(1+z) = 1$.

We emphasize once more that we have no a priori assumptions about the parametric form of the underlying data nor the relationship between luminosity and redshift.

Figure 3 shows the cumulative luminosity distribution $N(> L')$, for luminosities derived from the upper limit (dashed line) and lower limit (dotted line) to the $L - V$ relation. The luminosity functions for the “bounding” data are similar to one another, breaking at around 5×10^{51} ergs/s, as with the best fit value; however, the lower bound to the $L - V$ relation gives a more narrow luminosity function, while the upper bound broadens it relative to the best fit relation. Figures 5 and 6 show the cumulative and differential distributions, $N(< Z)$ and $dN/d\log Z$ respectively, for the bounding L-V relations. It is clear from Figures 5 and 6 that the lower bound (dotted line) to the $L - V$ relation places the large majority of bursts at relatively low redshifts (below $z \sim 4$), while the upper bound (dashed line) to the $L - V$ relation causes a disproportionate number of bursts to be located at $z \gtrsim 10$. In the remainder of this paper, we will utilize the nominal values of the luminosities and redshifts as derived in FRR. We also point out that the dependence on the choice of cosmological model is not a significant source of uncertainty (compared to the uncertainty from the scatter in the L-V relationship).

5. Discussion

5.1. On the Presence of Luminosity (or Jet Angle) Evolution

Under the assumption that the luminosity-variability correlation indeed produces valid redshifts for GRBs, the data show the presence of significant luminosity evolution (a $> 10\sigma$ correlation between L and $1 + z$) in which the average GRB luminosity scales as $(1 + z)^{1.4}$. Even when the slope of the underlying luminosity-variability relation changes (within the maximum bounds allowed by the 8 GRBs used to derive this relation), the correlation between GRB luminosity and redshift remains. It is important to address the question of the origin or meaning of this evolution. Because our variable L above is really $L/d\Omega$, where $d\Omega$ is the jet opening solid angle of the GRB, the correlation of L with redshift can result from the evolution of either L , or Ω or both. We discuss each in turn below.

5.1.1. Luminosity Evolution

If the correlation between $L/d\Omega$ and redshift is due to the evolution of the amount of energy per unit time emitted by the GRB progenitor (and not evolution of the jet opening angle), then this suggests that bursts were significantly brighter in the past. Presumably, this evolution is the result of a variation in the progenitor of the GRB. If the progenitors of GRBs are indeed massive stars, then somehow the distribution or structure of these massive stars must be different at high redshifts.

Currently, both observational and theoretical arguments (e.g. Larson, 1998, and references therein; see also Malhotra & Rhoads, 2002) suggest that the stellar initial mass function (IMF) was “top heavy” at high redshift - that is, the mass scale of the IMF was higher in the earlier stages of the universe. A time varying IMF with a higher mass scale at higher z is a very realistic possibility based on the following arguments from Larson, 1998: The mass scale in the IMF is likely to depend strongly on the temperature in star forming clouds. In the early universe, this temperature was probably higher for several reasons - the cosmic background temperature was higher, the metallicity was lower which implies lower cooling rates and therefore higher temperatures on average, heating rates were probably higher in the past because the star formation rate per unit volume was higher leading to more intense radiation fields at high redshifts (for further details, see Larson, 1998). The higher temperatures imply that a larger mass scale (e.g. Jeans mass) is required to collapse protostellar material and form a star. Because of these and other effects, Larson suggests that the mass scale of the IMF could have been as much as an order of magnitude or more higher at redshifts larger than 5.

In addition, since mass loss from stellar winds seems to depend on stellar metallicities (e.g. Meynet et al. 1994; Langer & Henkel 1995; Ramirez-Ruiz et al., 2000), these massive stars are less likely to lose much mass before collapse. At low redshift (roughly solar metallicities), even if these massive stars formed, they would lose most of their mass due to winds before collapse. So at higher redshift, the progenitors of GRBs are not only likely to form with higher average masses, but will also retain this mass until collapse.

One might expect that this increase in mass could lead to an overall larger energy budget and hence more luminous bursts at earlier times. For example, a fairly generic scenario for the engine which drives GRBs invokes the rapid accretion of a disk around a stellar-massed black hole (Popham, Woosley, & Fryer 1999). In such a scenario, the energy in the burst increases dramatically with amount of mass in, and accretion rate of, the disk (Popham et al. 1999). More massive progenitor stars tend to produce higher accretion rates and hence, stronger GRBs. In general, this is true whether the engine producing the burst is driven by neutrino annihilation or magnetic fields.

The simple argument of “more massive progenitor = more luminous GRB”, however, ignores much of the subtle physics required to produce a GRB from some cataclysmic event (such as a collapse to a black hole or some sort of compact object merger). For collapsar models, the *most massive* ($300M_{\odot}$) stellar progenitors may only produce weak or no relativistic outflows (Fryer, Woosley, & Heger 1999). Although the accretion rate on the black hole is much higher for these stars, the angular momentum is too low to produce a stable disk until most of the star has already accreted onto the black hole. The characteristics of a GRB outflow - particularly in these collapsar models - also depend on the density of the surrounding stellar envelope which the outflow must “punch” through, the accretion rate (which depends on many factors including the spin of the BH), the presence of magnetic fields, etc. Of course, the luminosity of the GRB outflow also relies on the mechanism and efficiency of energy extraction from the black hole, which (for example in a Blandford-Znajek mechanism; Blandford & Znajek, 1977; see Popham et al. 1999 for a review) can depend critically on the angular momentum as well as the mass of the black hole.

The relationship between progenitor mass and GRB energy output is therefore not straightforward for all progenitor models. *However, there are some situations in which this relationship holds very well.* If the specific angular momentum in the core of massive stars did not vary with stellar mass, then it is likely that more massive stars would produce more energetic bursts (MacFadyen & Woosley, 1999). For some black hole accretion disk models (e.g. He mergers), Zhang & Fryer (2001) have shown that the GRB energy does increase with increasing stellar mass. Therefore, depending on the model, it is possible that progenitor mass evolution (due to a top-heavy IMF) or core mass evolution (due to metallicity effects)

may be responsible for the observed luminosity-redshift correlation. But this is not the only possibility as we discuss below.

5.1.2. Jet Opening Angle Evolution

It was recently suggested (Frail et al., 2000; see also Panaiteescu & Kumar, 2001) that the GRB luminosity is in fact constant, and it is the jet opening angle that causes the dispersion in the apparent or isotropic equivalent GRB luminosity. This analysis relies on the fact that the break observed in many GRB afterglow light curves is due to a geometrical jet effect (Rhoads, 1997) and not, for example, a transition from a relativistic to non-relativistic phase (Huang, Dai & Lu, 2000) or environmental effects such as a sharp density gradient (Chevalier & Li, 2000; Ramirez-Ruiz et al., 2000). If the Frail et al. result is correct, then our results above imply the existence not of luminosity evolution, but dependence of the *jet angle* as a function of redshift. In this case, we trade L for $1/\Omega$ so that the jet solid angle Ω is proportional to $(1+z)^{-1.4}$; in other words, the average opening angle is expected to be smaller in the past⁷.

Physically, the evolution of the jet opening angle is a matter of speculation. The angle into which the baryonic/leptonic outflow is beamed is probably strongly dependent on, among a number of factors, the rotational velocity of the progenitor. For example, in the collapsar model of MacFadyen & Woosley (1999), a GRB is produced when a very massive star with angular momentum in a specified range (enough to prevent spherical collapse, but not too much to prevent collapse on a reasonable timescale) collapses to a black hole. Because the star is rapidly rotating, accretion is suspended along and around the equitorial plane. Thus, only matter along the rotation axis can fall into the black hole and evacuate a region to allow for reversal of flow - that is, outflow from the progenitor, which will produce the GRB jet. For higher rotational velocities, this evacuated region will be more collimated and thus have a smaller jet opening angle. Therefore, evolution of the progenitor rotational velocity (in which stars rotated more rapidly at higher redshifts) could at least qualitatively explain our results⁸. However, it is not at all clear how one might produce this type of evolution.

⁷Note that all of the distributions for L translate into distributions for $1/\Omega$ via a factor $\sim 10^{50}$ ergs, the Frail et al. standard luminosity.

⁸We point out that this model does not include MHD, which is also likely to play an extremely important role in the collimation of the jet.

5.1.3. Comparison with Other Luminosity Functions.

Not surprisingly, the luminosity functions of many astrophysical objects (e.g. galaxies, quasars, etc.) show signs of evolution with redshift. It is often a difficult task to quantify this evolution - observationally and theoretically - due to either numerous selection effects (e.g. dust, malmquist biases, sensitivity, etc.) which tend to plague the observations, or the presence of simplifying assumptions and lack of numerical resolution in the theoretical simulations. However, we can make some quantitative statements about the luminosity evolution of various astrophysical objects. For instance, it is fairly well established (Marzke et al. 1994) that the local luminosity function varies for early and late type galaxies; when parameterizing the luminosity function by the standard Schechter function, the power law index evolves from $\alpha = -0.8$ for early type galaxies to $\alpha = -1.8$ for late type galaxies (implying more luminous galaxies at earlier times). Fried et al. (2001) find that the luminosity evolution depends significantly on the galaxy type, and present a list of luminosity functions and their evolution for many galaxy types (see Table II in their paper). In the case of starburst galaxies, for example, the highest redshift galaxies are intrinsically brighter than the lowest redshift, but fainter than intermediate redshift. Numerical simulations of Nagamine et al. (2001) find that the characteristic luminosity of galaxies increases by 0.8 mag from $z = 0$ to 2 and then declines towards higher redshift, while the B-band *luminosity density* continues to increase from $z = 0$ to 5 (although only slowly after $z \sim 3$), for a Λ CDM universe. The quasar luminosity function also appears to evolve with redshift. The luminosity evolution is generally accepted as $L \sim (1 + z)^3$ for $z < 1.5$ and constant after that up to redshifts of 3 (Boyle, 1993; Hewett et al. 1993), although alternative models suggest $L \sim (1 + z)^{1.5}$ out to a redshift of 3 (Hewett et al., 1993).

Comparison of these luminosity functions with the GRB luminosity evolution is not straightforward because - as mentioned above - of the various selection effects that play a role in determining galaxy and quasar luminosity functions, not to mention the fact that it is unclear how one would physically connect the GRB to these types of luminosity functions. It would be perhaps most useful to compare our results for GRB luminosity evolution with that of different types of supernovae, because of the eminent link between GRBs and massive stars. Unfortunately, this will have to await the next generation of supernovae observations (such as SNAP), while the current data is insufficient to say anything about the evolution of supernovae luminosity to high redshifts. It should be emphasized again, however, that almost all astrophysical objects for which sufficient data exists have shown evidence of luminosity evolution, and its theoretical origin as well as observational consequences should be seriously investigated for GRBs.

5.2. The GRB Density Distribution and Estimating the Star Formation Rate at High Redshift

There has recently been a large volume of both observational and theoretical work suggesting GRBs are associated with massive stars. The observational evidence is based on colors and other properties of GRB host galaxies suggesting active star formation (Sokolov et al., 2001), burst locations in their host galaxies (Bloom et al., 2000), possible evidence of supernovae in the light curves of some afterglows (Bloom et al., 1999, Reichart, 2000), and the and direct iron line observations in the X-ray afterglows of a few GRBs (Piro et al., 2000 Antonelli et al., 2000)⁹. Theoretically, massive star progenitors have proved to be viable models particularly for the longer duration bursts (Woosley, 2000, MacFadyen & Woosley, 1999). If GRBs are indeed the final episode in a single massive star’s life, then the rate density of GRBs will be strongly correlated with the overall star formation rate. Other progenitors such as binary mergers will also show evidence of such a correlation, although the correlation is not as straightforward (see §5.2.1 below; see also Fryer, Woosley, & Hartmann, 1999). Other arguments linking GRBs with massive stars can be found in Totani (1997), Blain & Natarajan (2000), Lamb & Reichart (2000), and Ramirez-Ruiz, Trentham, and Blain (2001).

Therefore, GRBs are in principle ideal tools for constraining the star formation rate, which has been one of the most important problems in extra-galactic astrophysics for decades. One of the advantages of using GRBs to trace the SFR is that the gamma-rays and X-rays from the burst travel from the source to our telescope relatively unhindered and so are not subject to the types of selection effects present in the UV and Far-IR methods of determining the SFR (see Schaefer, 1999, for a review). Indeed using the luminosity-variability correlation to determine redshifts relies on the gamma-ray data, which avoid selection effects present in lower energy bands. Furthermore, because GRBs may exist out to redshifts $z \geq 10$ if they can be associated with the earliest population of massive stars, they can probe the SFR to higher redshifts than any other method used previously (see also Lamb & Reichart, 2000).

In Figure 7, we have plotted the co-moving rate density distribution as a function of redshift for an $\Omega_\Lambda = 0.7$, $\Omega_M = 0.3$ universe. First, we note that there is an increase in the rate density $\sim (1+z)^3$ out to a redshift of $(1+z) \sim 3$. Although there are relatively few bins or points here, this is similar to independent determinations of the star formation rate to

⁹We point out, however, that some studies of extinction in the light curves of GRBs (e.g. GRB000926) show a different extinction than what is expected for young star forming regions (Price, et al., 2001). In addition, Tsvetkov et al. (2001) find that there is a small probability (4%) that GRBs and star forming sites belong to the same region.

this redshift using various methods (as well as a “meta-analysis” of the SFR combining the various methods; see Hogg, 2001 and references therein). Beyond a redshift of $(1+z) = 3$, the GRB rate density flattens, although continues to rise as $\sim (1+z)^1$ until at least a redshift of 10, beyond which our sample is truncated. The very large portion of the co-moving rate density at high redshift may be evidence of a sample of population III stars. In the following section, we address the issues involved with associating the GRB rate density to that of the star formation rate, and then make estimates of the SFR based on different progenitor models for GRBs.

5.2.1. *Estimating the Star Formation Rate from the GRB Rate*

As mentioned above, most gamma-ray burst models are connected to the formation of massive stars and for some mechanisms, it is likely that the gamma-ray burst rate traces the SFR in the universe (Fryer, Woosley, & Hartmann 1999). However, as we probe increasingly higher redshifts, we find that metallicity dependent effects (mass loss from winds, slope of the initial mass function) can change the number of GRBs produced for a given amount of star formation (especially for the collapsar model which arise from only the most massive stars). In addition, the delay between stellar formation and merger for compact merger scenarios (double neutron star, black hole/neutron star) produces a detectable shift at high redshift.

To extract a star formation rate at high redshift from the gamma-ray burst distribution, we must not only know which progenitor(s) produce gamma-ray bursts, but how the evolution of these progenitors varies with increasing redshift. Although deriving an exact star formation rate is impossible at this time because of uncertainties (such as rotation rates of massive stars or neutron star kicks), with a few assumptions we can place some interesting limits on the star formation history using gamma-ray bursts. At one extreme, we take the collapsar model whose rate of formation for a given star formation rate increases dramatically with redshift, both because the amount of wind mass-loss decreases and because the initial mass function flattens at high redshift. At the other extreme, we consider the double neutron star and black hole-neutron star mergers which, because of the delay in their merging, produce fewer bursts for a given star formation rate at high redshift.

For both model scenarios (collapsers and binary mergers), we assume that mass loss from winds and the effects of the initial mass function are the only redshift dependencies on stellar evolution. For the collapsar model in particular, we are assuming that the rotation rate of a star at collapse does *not* depend on redshift and that the structure of the core depends only on mass loss metallicity effects. Stellar evolution models confirm the latter assumption, but too little is understood about rotation to judge our first assumption at this

time. For binary merger scenarios, we assume that the kick imparted onto neutron stars and black holes at birth does not vary with redshift.

For mass-loss, we assume that the mass loss rate (\dot{M}_{Winds}) depends on the metallicity:

$$\dot{M}_{\text{Winds}} \propto z_{\text{metal}}^{0.5}, \quad (9)$$

where z_{metal} is the metallicity (in units of solar metallicity). For the metallicity as a function of redshift (z), we are guided by the distribution from Pei, et al. (1999):

$$z_{\text{metal}} = \begin{cases} 10^{-0.5z} & \text{for } z < 3.2 \\ 10^{-0.8-0.25z} & \text{for } 3.2 < z < 5.0 \\ 10^{-0.2-0.4z} & \text{for } z > 5.0 \end{cases}$$

Given the metallicity as a function of redshift, we can determine the mass loss rate from equation 9. Unfortunately, the crucial parameter in calculating the formation rate of gamma-ray burst progenitors is the total mass lost, not the mass loss rate. Because mass loss alters the lifetime and luminosity of the star, the total mass loss, ΔM_{Total} does not scale linearly with the mass loss rate. Depending on the stellar model, $\Delta M_{\text{Total}} \propto \dot{M}_{\text{Winds}}^x \propto z_{\text{metal}}/2$ where x lies somewhere between 0.2-2.0 (e.g. Meynet et al. 1994; Langer & Henkel 1995). From Meynet et al. (1994), we see that for a $40M_{\odot}$ star, the total mass lost to winds does not decrease significantly ($x \approx 0$) until the metallicity drops below one half of solar, at which point it drops dramatically ($x \approx 0.5$ at $z_{\text{metal}} = 0.2$ and $x \gtrsim 1.0$ at $z_{\text{metal}} < 0.1$). For our calculations, we assume that $x = 0$ for metallicities above one half solar. At lower metallicities, we use a range of values for x to determine the dependence of the collapsar rate on this uncertain quantity (see Figure 8). The dependence of mass loss on metallicity is the dominant uncertainty in our calculations. In general, at any given redshift, there will be a distribution in metallicities which will tend to dilute the effects of metallicity variation as a function of redshift. However, as we see in Figure 8, this dilution only significantly alters the formation rate at low redshifts ($z < 1$) and is not crucial for our study of the high redshift star formation rate¹⁰.

The last effect that we include is the flattening of the initial mass function at high redshifts. It has long been thought that the first generation of stars (so-called population III stars) had an initial mass function skewed to more massive members (e.g. Silk 1983; Carr & Rees 1984; see also §5.1.1). To test the limits of this, we assume that population III stars dominate the stars formed above a redshift of 5 and that the initial mass function flattens

¹⁰However, if the mass loss rate remains relatively flat down to metallicities of one tenth solar or lower, metallicity effects can be important at high redshifts.

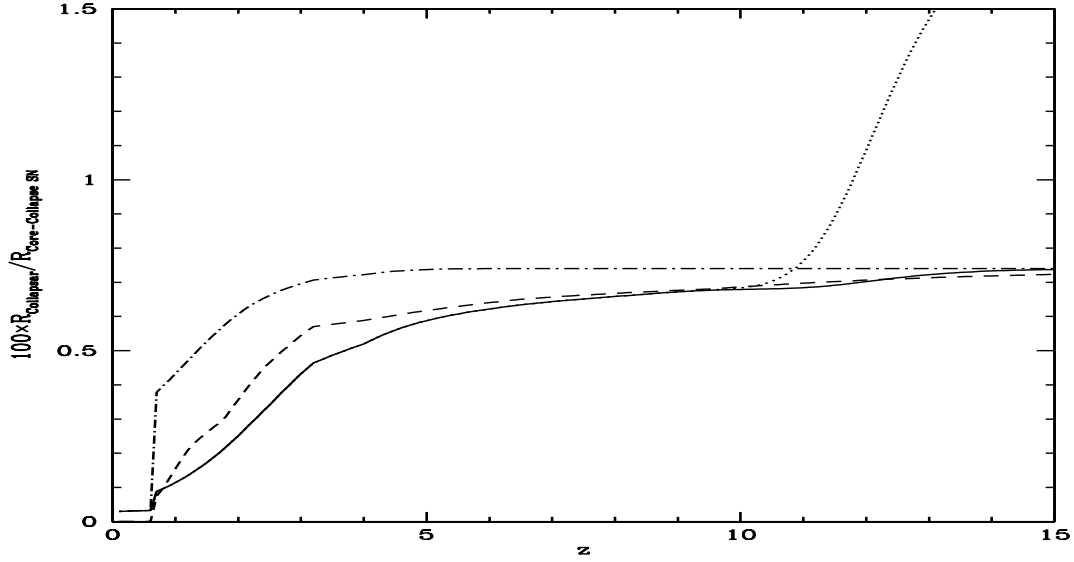


Fig. 8.— Collapsar rate as a function of redshift. The solid line assumes that the IMF does not change with redshift, but that mass loss from winds does change with metallicity: $x = 0$ above half solar metallicity and $x = 0.5$ at high redshift when the metallicity is below 1/2 solar (see §5.1 for details). For the solid line, the metallicity at a given redshift is given as a gaussian with a $1 - \sigma$ deviation set to 0.5 in the log of the metallicity. The dashed line gives the rate as a function of redshift without any spread in metallicity. The main effect of the spreading occurs at low redshift. The dotted line is identical to the solid line, but the IMF is flattened for population III stars. The dot-dashed line is the rate if we assume the mass loss changes more abruptly below 1/2 solar metallicities ($x = 2$).

from a steep IMF ($f(M) \propto M^{-2.7}$, where M denotes mass) at low redshift to a very flat IMF ($f(M) \propto M^{-1.5}$) for redshifts above 5. The effect of this IMF flattening on the collapsar rate is shown in Figure 8.

Figure 9 shows the co-moving rate density derived from both sets of progenitor models (using our results from the “best-fit” L-V relation). We have assumed that that x , the metallicity dependence, is 0,0.5 for respective metallicities above, below one-half solar. We have also assumed that there is a Gaussian spread in the metallicity (with a $1 - \sigma$ deviation set to 0.5 in the log of the metallicity). The solid and dotted lines in Figure 9 correspond to with and without the effects of a flattening IMF in the collapsar model. This provides a lower-limit for the slope of the SFR (with the best-fit data). The dashed and dot-dashed lines correspond, respectively, to the same models (with and without IMF flattening) for the compact merger models. These merger models provide a rough upper limit for the SFR

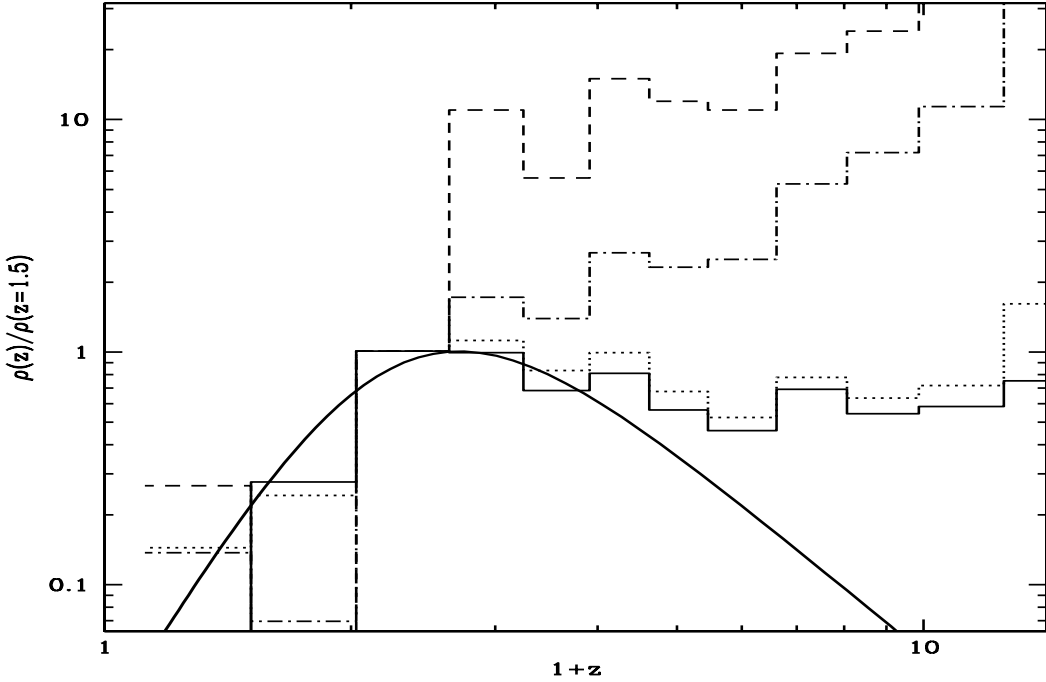


Fig. 9.— Estimates of the star formation rate based on various progenitor models. The solid and dotted lines correspond to the collapsar model, with and without the effects of a flattening IMF respectively. This provides a lower-limit for the slope of the SFR (with the best-fit data). The dashed and dot-dashed lines correspond, respectively, to the same models (with and without IMF flattening) for the compact merger models. We have superposed on the plot the star formation rate (SFR) from Blain (2001; dark solid line) which includes contributions to the SFR from both the UV and the sub-mm wavelength range.

derived from the rate of GRBs (He-merger and supernova GRBs will lie somewhere between the collapsar and compact merger burst models). For reference, we have superposed on the plot the star formation rate (SFR) from Blain (2001; dark solid line) which includes contributions to the SFR from both the UV and the sub-mm wavelength range (the latter contribution from the reprocessed UV emission absorbed and re-emitted by dust in the IR).

These calculations show the great potential that GRBs have for understanding the SFR at high redshifts. Understanding the progenitors of GRBs allows us to extract firm lower limits on the star formation history at high redshifts. Assuming the current best fit for the L-V relation, we find that the co-moving rate density does not decrease significantly with increasing redshift, and it may even increase.

These studies also provide evidence that compact mergers can not explain all GRBs. To explain the number of high-redshift merger GRBs (which require a lot of quickly merging compact binaries), our models tended to overproduce the number of GRBs that occur at low redshifts. If the rate of GRBs continues to increase at high redshifts as our results suggest, and if there is not some redshift dependence on the compact object kick magnitude, we can rule out compact merger models as the sole source of gamma-ray bursts.

6. Summary and Conclusions

Presently, there are ~ 20 gamma-ray bursts with directly measured redshifts. And although we have learned a remarkable amount from these few bursts, we still know very little about the GRB luminosity function and density distribution - two very important pieces in the GRB puzzle. Recently, it has been suggested (Norris et al., 2000; Fenimore & Ramirez-Ruiz, 2000; Reichart et al., 2000) that certain GRB observables can be used as “standard candles” or luminosity indicators from which to infer luminosities and redshifts. In particular, Fenimore & Ramirez-Ruiz (2000; FRR) have shown, using 8 bursts with measured redshifts, that there is a significant correlation between the luminosity of a GRB and the variability of its light curve (the “L-V relationship”). Using variability measurements from the light curves of 220 BATSE bursts, they used the L-V relation to compute a luminosity and (with knowledge of the observed flux and assuming a cosmological model) redshift for each burst.

In this paper, we have analyzed the FRR sample of 220 luminosities and redshifts. Because the FRR sample has a flux limit of $1.5\text{ph}/\text{cm}^2/\text{s}$, there is a strong truncation in the luminosity- redshift plane, which makes it difficult to directly determine the underlying luminosity and redshift distributions of the parent burst population. We have used well developed non-parametric statistical techniques to account for this selection effect. Our main results are as follows:

- **We have shown that there exists a significant correlation between the luminosity of a GRB and its redshift**, which can be parameterized by $L \propto (1+z)^{1.4 \pm \sim 0.5}$. This result is not very sensitive to the exact parameterization of the luminosity-variability correlation - when taking the extreme values for the power law indices of the the L-V relation or when drawing from a distribution of luminosities (spanning the range allowed by the L-V relation), we still find strong luminosity evolution, although with slightly different redshift dependence. If the L-V relation does indeed produce valid luminosities and redshifts for GRBs, then the evolution of GRB luminosity with redshift is a very robust result.

- We have estimated the GRB luminosity function *with the redshift dependence removed*, $\phi(L') = \phi(L/(1+z)^{1.4})$. We find the luminosity function has an average power law index of about -1.3 , and an apparent break at about $L' = 5 \times 10^{51} \text{ ergs}$. We also estimate the total luminosity emitted as a function of redshift and find that this quantity increases strongly with redshift (due not only to the large number of sources at high redshift, but also the strong correlation between luminosity and redshift).
- Accounting for the correlation between luminosity and redshift, we have estimated the co-moving rate density, $\rho(1+z)$, of GRBs in this sample. We find that ρ increases $\sim (1+z)^3$ until a redshift $1+z \sim 3$, consistent with star formation density results to this redshift (see Hogg et al., 2001). **Remarkably, the GRB rate density continues to increase as $\sim (1+z)^1$ until a redshift of $(1+z) \sim 10$** , beyond which our sample truncates.
- From the GRB redshift distribution, we have used the population synthesis codes of Fryer et al. (1999) to compute an estimate of the star formation rate at high redshifts. **We find that the star formation rate increases or remains constant to very high redshifts, no matter what the progenitor model.** We also find because our GRB rate density increases to high redshifts, merger models - which tend to overproduce GRBs at low redshifts - cannot be the sole source for all GRBs.

In this paper, we have also speculated on the possible origin of the luminosity evolution, and compared it to other known sources of luminosity evolution. The evolution we observe may be due to either an evolving energy output of the GRB progenitor or a changing jet opening angle with redshift. We have discussed some possible scenarios for each type of evolution; particularly, a top-heavy IMF may be responsible for producing more massive BH cores of collapsed stars and high redshift and this may lead to more energetic bursts. These speculations need to be examined in further detail.

We emphasize again that our results rely on the existence of the L-V relation and its ability to give correct luminosities and redshifts. Future redshift measurements will help confirm and more quantitatively establish this relationship. However, a true test of our results will have to await the Swift satellite, which is expected to get redshifts to hundreds of bursts over a few years. With a good handle on the selection effects of the detector, multi-wavelength GRB observations will not only provide us with a multitude of redshifts and luminosities, but will help us constrain the GRB environment and hopefully help elucidate the source of the luminosity evolution, and its relationship to the GRB progenitor(s).

Acknowledgements: We are very indebted to Ed Fenimore for providing unpublished tables of redshifts and luminosities from the FRR paper. We also are grateful to an anonymous referee whose comments led to many clarifications in this paper. N.L-R. and C.L.F.

would like to thank the Aspen Center for Physics for their hospitality and for providing a good working environment where some of this work was carried out. We would also like to thank Vahe' Petrosian, Don Lamb, Andrew MacFadyen, Shiho Kobayashi, for useful discussions. N.L.-R. acknowledges support from NASA grant NAG5-7144. The work of C.L.F. was funded by a Feynman Fellowship and an in-house ASCI grant at LANL. E.R.-R. acknowledges support from CONACYT, SEP and the ORS foundation, and would like to thank A. Blain, D. Lazzati, P. Natarajan & N. Trentham for helpful conversations.

REFERENCES

Antonelli, L.A., et al. 2000, ApJ, 545, L39

Beloborodov, A.M., et al. 2000, ApJ, 535, 158

Blain, A.W. & Natarajan, P. 2000, MNRAS, 312, L35

Blain, A.W. 2001, in “Starburst Galaxies: Near and Far”, 2001, L.Tacconi & D. Lutz eds., Springer: Berlin, p. 303.

Blandford, R.L. & Znajek, R.D. 1977, MNRAS, 179, 433

Bloom, J.S., et al. 1999, Nature, 401, 453

Bloom, J.S., et al. 2000, AJ, in press; (astro-ph 0010176)

Boyle, B.J. 1993, in The Environment and Evolution of Galaxies, Shull J.M., Thronson H.A., eds, Kluwer, Dordrecht, p. 433

Carr, B.J. & Rees, M.J. 1984 MNRAS, 206, 315

Chevalier, R.A. & Li, Z.Y. 2000, ApJ, 536, 195

Efron, B. & Petrosian, V. 1992, ApJ, 399, 345

Efron, B. & Petrosian, V. 1999, JASA,

Fenimore, E.E., et al. 1995, ApJ, 448, L101

Fenimore, E.E & Ramirez-Ruiz, E. 2000, submitted to ApJ (astro-ph 0004176)

Frail, D.A., et al. 2001, ApJ, 562, L55

Fried, J.W., et al. 2001, A&A, 367, 788

Fryer, C.L., Woosley, S.E., & Hartmann, D.H. 1999, *ApJ*, 526, 152

Fryer, C.L., Woosley, S.E., & Heger, A. 2001, *ApJ*, 550, 372

Hewett, P.C., et al. 1993, *ApJ*, 406, 43

Huang, Y.F., Dai, Z.G., & Lu, T. 2000, *MNRAS*, 316, 943

Ioka, K. & Nakamura, T. 2001, *ApJ*, 554, L163

Kobayashi, S., et al. 1997, *ApJ*, 490, 92

Lamb, D.Q. & Reichart, D.E. 2000, *ApJ*, 536, 1

Langer, N., & Henkel, C. 1995, *Space Science Reviews*, 74, 343

Larson, R.B. 1998, *MNRAS*, 301, 569

Lloyd, N.M. & Petrosian, V. 1999, *ApJ*, 511, 550

Lloyd, N.M., et al. 2000, *ApJ*, 534, 227

Lyden-Bell, D. 1971, *MNRAS*, 155, 95

MacFadyen, A. & Woosley, S.E. 1999, *ApJ*, 524, 262

Madau, P., et al. 1998, *ApJ*, 498, 106

Malhotra, S. & Rhoads, J.E. 2002, *ApJ*, 565, L71

Maloney, A. & Petrosian, V. 1999, *ApJ*, 518, 32

Marzke, R.O., et al. 1994, *AJ*, 108, 437

Meynet, G., Maeder, A, Schaller, G., Schaerer, D., & Charbonnel, C. 1994, *A&A*, 103, 97

Meszaros, P. 2001, *Science*, 291, 79

Nagamine, K., et al. 2001, *MNRAS*, 327, L10

Norris, J.P., Marani, G.F, Bonnell, J.T. 2000, *ApJ*, 534, 248

Panaitescu, A. & Kumar, P. 2001, *ApJ*, 554, 667

Pei, Y.C., Fall, S.M., & Hauser, M.G. 1999, *ApJ*, 522, 604

Petrosian, V. 1993, *ApJ*, 402, L33

Piran, T. 1999, Physics Reports, 314, 575

Piro, L., et al. 2000, Science, 290, 955

Plaga, R. 2001, A&A, 370, 351

Popham, R., Woosley, S.E., & Fryer, C.L. 1999, ApJ, 518, 356

Price, P.A., et al. 2001, ApJ, 549, L7

Ramirez-Ruiz, E., et al. 2001, MNRAS, 327, 829

Ramirez-Ruiz, E., Trentham, N., & Blain, A.W. 2002, MNRAS, 329, 465

Ramirez-Ruiz, E. & Lloyd-Ronning, N.M. 2002, New Astronomy, submitted.

Reichart, D.E., et al. 2000, ApJ, 552, 57.

Reichart, D.E. 2000, ApJ, 521, L111

Rhoads, J.E. 1997, ApJ, 487, L1

Schaefer, B.E. 2001, submitted to ApJL, (astro-ph 0101462)

Schaerer, D. 2000, to appear in "Building the Galaxies: from the Primordial Universe to the Present", F. Hammer et al. eds, (astro-ph 9906014)

Schmidt, M. 2001, ApJ, 552, 36

Silk, J. 1983, MNRAS, 205, 705

Sokolov, V.V., et al. 2001, A&A 372, 438

Totani, T. 1997, ApJ, 486, L71

Tsvetkov, D.Y., et al. 2001, in "Strongest Explosions in the Universe", SAI, Moscow (astro-ph 0101362)

Woosley, S.E. 1993, ApJ, 405, 273

Woosley, S.E. 2000, in Gamma Ray Bursts, AIP Conf. Proc. 526, eds R.M. Kippen, R.S. Mallozzi, G.J. Fishman, p. 555

Zhang, W. & Fryer, C.L. 2001, ApJ, 550, 357